

X-ray photoelectron studies of thorium, uranium, and their dioxides*

B. W. Veal and D. J. Lam

Argonne National Laboratory, Argonne, Illinois 60439

(Received 20 May 1974)

The valence-band structures of the light actinides thorium, uranium, and their dioxides have been investigated by means of x-ray photoemission spectroscopy. This study shows that the electronic structures of ThO_2 and UO_2 are quite similar, except for the presence of $5f$ electrons in UO_2 which lie close to the Fermi level. It is these low-binding-energy $5f$ electrons that give rise to the most dramatic differences in physical properties, notably the magnetism, electrical conductivity, and color. Conduction in UO_2 apparently occurs via holes created by excitation of rather localized $5f$ electrons from the uranium to interstitial oxygen-acceptor sites. Sputtering experiments on thin oxide film and bulk samples show Fermi-level shifts in x-ray photoemission spectra associated with doping changes that result from preferential removal of interstitial ("impurity") oxygen atoms. The deep-trap and polaron conduction models have been reexamined. It is our view, at this time, that neither model can be ruled out. For the pure metal thorium, valence-band spectra were compared with the available density-of-states calculations and satisfactory agreement was obtained. For α -uranium, no detailed band calculation exists. However, the results agree with the qualitative density-of-states picture presented by Friedel.

I. INTRODUCTION

The actinide series, consisting of those elements heavier than radium, is a transition series in which the $5f$ -electronic states become filled. The actinides are analogous to the lanthanides, where $4f$ -electron occupation begins. In the lanthanides,¹ the $4f$ electrons are relatively well understood. However, little is known about the nature of the $5f$ electrons in the actinides, and the interpretation of the observed electric, magnetic, and optical properties remains somewhat obscure. Thorium is thus far the only metal in the actinide series for which experimental data exist that relate the detail of the electronic structure and the Fermi surface.^{2,3} Unfortunately, the electronic structure of thorium metal has no occupied states of f character so that Fermi-surface data were unable to delineate the role and nature of the $5f$ electrons.

Thorium, at the beginning of the actinide series, has a $6d^2 7s^2$ free-atom electronic configuration, and the metal has a face-centered-cubic structure at room temperature. The free-atom electronic configuration of uranium is $5f^3 6d^1 7s^2$, and the room-temperature allotrope has an orthorhombic crystal structure. Since thorium contains no occupied $5f$ states and uranium does have $5f$ occupation, the elements thorium and uranium (and their respective compounds) provide good comparative systems for investigating the role of $5f$ electrons.

Thorium dioxide is a stable diamagnetic compound and is a wide-gap transparent insulator with a melting point of 3600 °K. Uranium dioxide is also a refractory oxide with a melting point of 3200 °K.⁴ However, UO_2 is a colored (brown

to black) semiconductor and exhibits antiferromagnetism with a Néel point of 30 °K.^{5,6} Both ThO_2 and UO_2 occur in the CaF_2 crystal structure. Thorium dioxide forms stoichiometrically, whereas UO_2 tends to form hyperstoichiometrically, with excess oxygen at interstitial lattice sites.⁷ Detailed magnetic studies on UO_{2+x} indicate that the magnetic susceptibility decreases with an increase in oxygen concentration.⁵ The magnetic-susceptibility results were interpreted in terms of U^{5+} or U^{6+} ions replacing U^{4+} ions in the uranium sublattice with the introduction of excess interstitial oxygen in the stoichiometric UO_2 lattice. Data obtained from electrical-transport properties of single-crystal⁸ and polycrystalline^{9,10} UO_2 were interpreted both in terms of a band model and a simple ionic model.

The technique of x-ray photoelectron spectroscopy (XPS), which can provide a direct picture of the occupied electronic bands in metals, alloys, and compounds, has been applied to study the occupied electronic states of uranium and thorium oxides by several investigators.¹¹⁻¹³ Most of this work was concerned with chemical shifts of the uranium $4f$ levels in different atomic environments. Recently, Fuggle *et al.*¹⁴ reported valence-band and core-level XPS spectra for clean and oxidized thorium and uranium surfaces. They found large discrepancies between their measurements of several uranium core-level energies and the previously reported energies. Their valence-band spectra show some of the features that we are reporting. However, because of resolution or other limitations, they were unable to discern the behavior of the $5f$ electrons in these materials.

In the present paper, XPS spectra are reported for the metals thorium and α -U as well as ThO_2

and UO_2 . For UO_2 , we have seen excitation spectra in which the $5f$ -electron states can be specifically identified and located in relation to the remaining valence-band electrons. The results provide new insight into the conductivity mechanism in UO_2 , a process that has not been well understood.

II. EXPERIMENTAL PROCEDURE

The XPS spectra were obtained with a Hewlett-Packard 5950A spectrometer using a monochromatized aluminum x-ray source with a resolution of ~ 0.5 eV. The vacuum in the measuring chamber of the instrument was in the low 10^{-9} -Torr range. The spectrometer was equipped with an ion-sputtering gun for sample cleaning, and a low-energy-electron flood gun for neutralization of surface charge buildup in insulators. The spectra were obtained from bulk polycrystalline ThO_2 obtained from a commercial source and from an oxidized thorium metal surface. Since the bulk ThO_2 samples could not be cleaned *in situ*, all of the ThO_2 data presented in this paper were taken from the thin surface-film rather than sintered bulk samples. Such films should be suitably characterized since only one oxide of thorium can be stabilized. In any case, except for identifiable contaminants in the bulk sample, the film and bulk spectra were the same. Spectra of UO_2 were obtained from a bulk sintered sample with a composition of $\text{UO}_{2.008}$ and from the oxidized surface of uranium metal. No significant differences were found between bulk and film UO_2 samples.

Spectra of thorium and uranium metals were obtained using bulk samples that were cleaned by dc sputter etching with argon ions. The etching was done in a sample preparation vacuum chamber attached to the XPS instrument. The sample was moved between the preparation chamber and the "run" chamber with a sample insertion rod isolated from the atmosphere with Teflon sliding seals. A burst of gas was always observed in the preparation chamber when the sample was inserted. Thus some surface contamination was inevitable. Furthermore, the oxide contaminant line monitored on the thorium- and uranium-metal spectra could be seen to grow while XPS spectra were being recorded. The oxide growth rate for both metals was relatively slow so that, after about 20 h of run time, the spectrum was still predominately that of the metal. The "cleanest" α -U spectrum was obtained by adding together seven runs of ~ 6 min duration obtained under maximum x-ray power. Data were recorded and the sample was etched in alternate sequence until adequate statistics were obtained. For thorium metal, the spectrum was recorded in a single run after sputter cleaning.

Since ThO_2 is a good insulator, positive charge buildup on the bulk sample surface results from electron depletion during the XPS measurements. This electron depletion results in a severe shift of the entire spectrum with attendant line broadening. Consequently, the sample was "neutralized" by flooding with low-energy electrons supplied by a filament located in close proximity to the sample.¹⁵ The electrons generated by the filament are accelerated by a grid, so that this charge-compensation device may result in a slight negative charge buildup on the sample during measurement. The buildup can apparently be calibrated by looking at the "flooded" oxide spectrum and comparing it with the spectrum of a thin oxide layer grown on the conducting-metal substrate (no shift of the thin-film spectra is observed when the sample is flooded with low-energy electrons). Furthermore, for a fixed setting of the flood-gun control, the same calibration is obtained in a similar experiment with aluminum and Al_2O_3 .

According to the measurements of Nagels *et al.*,⁸ the sample of UO_2 that we used should be a moderately good room-temperature conductor ($\rho \sim 1000 \Omega \text{ cm}$). We would therefore not expect charge buildup on the sample during the photoemission measurement and, in fact, no shift was observed with application of the electron flood gun.

III. RESULTS AND DISCUSSION

A. Thorium and α -uranium metals

XPS spectra of thorium were recorded using a bulk sample that was cleaned by dc sputter etching with argon ions. Although it was impossible for us to obtain a completely oxygen-free thorium surface, we were able to obtain samples with no more than a few monolayers of oxide contaminant. Thus a strong metal spectrum superimposed on the ThO_2 spectrum was obtained. Figure 1 shows the cleanest thorium-metal sample we were able to obtain (lower spectrum) and also the oxide-film spectrum (upper curve). Similar results were obtained by Fuggle *et al.*¹⁴ on vapor-deposited thorium metal, which was prepared and measured in high vacuum and subsequently oxidized at the metal surface. However, they were able to obtain an XPS spectrum of thorium metal with less oxygen contamination.

From examination of Fig. 1, we see that the metal valence-band spectra, which intersect the Fermi level E_F , are well separated from the valence electrons that make up the metal-oxide bond in ThO_2 . Thus the presence of the contaminant-oxide spectra does not distort the shape of the metal valence-band spectrum and can easily be subtracted from the composite spectrum.

Electronic band-structure calculations for thorium metal have been reported by Gupta and

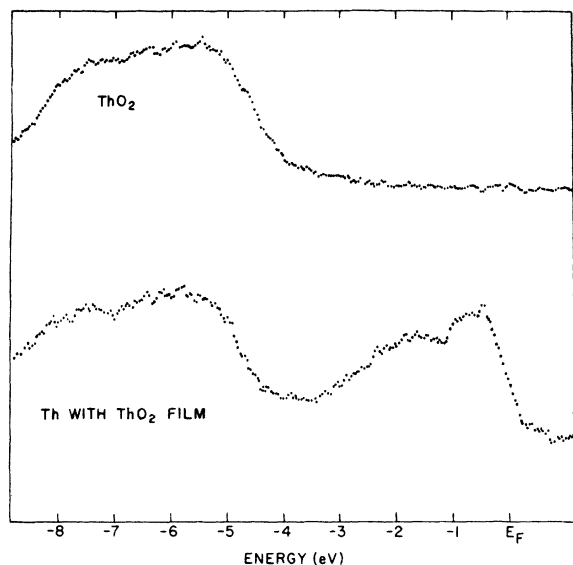


FIG. 1. XPS spectra of ThO₂ (upper spectrum) and thorium metal with ThO₂ contaminant (lower spectrum).

Loucks¹⁶ and by Koelling and Freeman.¹⁷ Both calculations have been able to predict all the observed Fermi-surface areas found in de Haas-van Alphen experiments. Both give quite similar valence-band densities of states. Figure 2 shows a comparison between the valence-band XPS spectrum and the band calculation of Freeman and Koelling.¹⁸ In this figure, the theoretical results were broadened with a 0.55-eV full width at half-maximum Gaussian function to simulate the instrument resolution function. No correction was made for the small experimental background resulting from inelastically scattered electrons. The agreement between theory and experiment is quite good, ex-

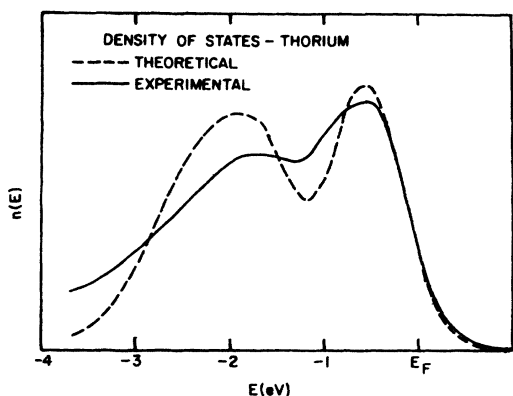


FIG. 2. Comparison between the XPS spectrum and the theoretical density-of-states curve for thorium metal.

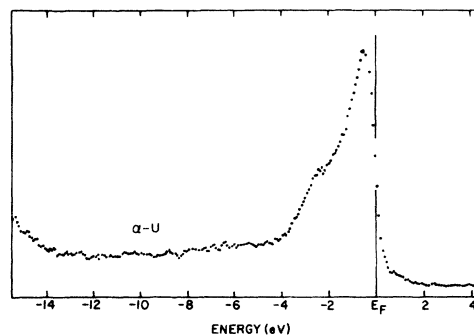


FIG. 3. XPS valence-band spectrum of α -uranium. The weak shoulder near -2 eV may result from oxygen contamination.

cept at the high-binding-energy side of the spectrum. Substantially more broadening occurs at this energy in the experiment than in the theory. This broadening of valence-band spectra at energies remote from E_F is a frequently recurring observation for metal XPS spectra.¹⁹ Presumably we are observing an energy-dependent broadening phenomenon that is outside the realm of one-electron theory.

The XPS valence spectra for α -uranium are shown in Fig. 3. Unlike thorium, the uranium-metal valence-band spectra are not well separated from the oxide spectra. Since the oxide could not be completely removed from the metal and since the oxide spectra shift in energy relative to E_F with decreasing film thickness, the derived valence-band spectrum is uncertain as a result of a small, but not easily determinable, contribution from the oxide film. This uncertainty is most prominent in the vicinity of the small shoulder near -2 eV. More discussion on this point will be given in Sec. III B.

No detailed comparison can be made between theory and experiment, since the theory has not been adequately developed.²⁰ However, the XPS results are consistent with the qualitative band picture of α -uranium suggested by Friedel.²¹ Using magnetic-susceptibility, specific-heat and thermoelectric-power data, Friedel inferred band structures for the α , β , and γ phases of uranium metal. The form of the valence band suggested for α -uranium consists of a narrow band that contains four electrons per atom and is derived from hybridized 5*f* and 6*d* orbitals. The two remaining electrons form a broader band derived from 7*s* orbitals hybridized with 5*f* and 6*d* orbitals. The band that contains four electrons should start about 0.3 eV below the Fermi level.

It is difficult to compare the XPS spectra of α -uranium with that derived from one-electron

band theory since the XPS electron yields are significantly affected by the angular momentum quantum number l .²² The l -dependent transition rates are quite important to the valence-band spectra of α -uranium, in which the bands are an admixture of s , p , d , and f electrons. We should expect our XPS measurement to show significant distortion from the ground-state density of states by displaying strong enhancement of the f -electron character. A calculation of the transition-rate correction should be performed before making detailed comparisons with band theory.

B. ThO_2 and UO_2

The XPS spectra of UO_2 and ThO_2 within 45 eV of the Fermi level E_F are shown in Fig. 4. The prominent narrow peak near E_F in the UO_2 spectrum must be attributed to the uranium $5f$ electrons. In both UO_2 and ThO_2 , the "bonding" band, which consists of metal $6d$ and $7s$ electrons bonded with oxygen $2p$ electrons, is centered at ~ 6 eV below E_F . The uranium $6p_{3/2}$ and $6p_{1/2}$ peaks are located at 18 and 28.5 eV below the Fermi level, respectively. These values are close to those obtained by Fuggle *et al.*¹⁴ The oxygen $2s_{1/2}$ spectrum occurs at 23 eV. The oxygen $2p$, which is 16 eV apart from the $2s_{1/2}$, can be recognized within the valence band. [This 16-eV separation between the $\text{O}(2p)$ and the $\text{O}(2s_{1/2})$ observed in both UO_2 and ThO_2 is also found in numerous transition-metal oxides.²³] The thorium $6p_{3/2}$ and $6p_{1/2}$ doublet peaks are located at 17.3 and 26 eV, respectively, from the Fermi level. For the insulator ThO_2 , the Fermi level is, of course, not defined during the XPS measurement because of nonequilibrium conditions. However, because the data were taken on a thin oxide film grown on a bulk thorium-metal substrate, no spectral shifts due to charge build-up were observed. Thus no arbitrary shift of the ThO_2 spectra relative to UO_2 was necessary for the

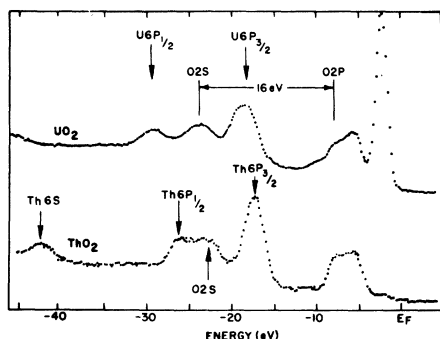


FIG. 4. XPS spectra of UO_2 and ThO_2 within 45 eV of the Fermi energy. The narrow peak in UO_2 near E_F is associated with the $5f$ electrons.

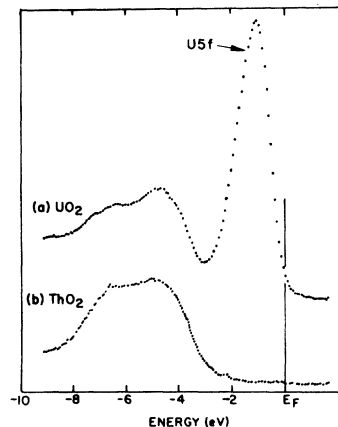


FIG. 5. XPS valence spectra of UO_2 and ThO_2 . The strong similarity between the bonding bands of these two oxides provides for easy identification of the $5f$ electrons in UO_2 . The near proximity of the $5f$ electrons to E_F implies that they are responsible for the conductivity and color of UO_2 .

data shown in Figs. 4 and 5. Again, these energies are nearly identical to those obtained by Fuggle *et al.* The thorium $6s_{1/2}$ spectrum can be observed at 43 eV below the Fermi level, whereas the uranium $6s_{1/2}$ line is outside the energy range we scanned.

Except for the existence of the $5f$ -electron spectrum in UO_2 , ThO_2 and UO_2 valence-band spectra are nearly indistinguishable (Fig. 5). Thus we expect the most profound differences in the two oxides (notably, the conductivities, color, and magnetism) to be directly related to the $5f$ electrons present in UO_2 and missing in ThO_2 .

The optical gap in ThO_2 , determined by optical transitions from the "bonding" band to the conduction-band minimum, is approximately 6 eV.²⁴ For UO_2 , the energy gap between the $5f$ states near E_F and the conduction-band minimum is ~ 2.7 eV, as determined by optical-absorption²⁵ and high-temperature electrical-conductivity⁹ measurements. From Fig. 5, however, we see that the separation between the leading (low-binding-energy) edges of the $5f$ peak and the bonding band is ~ 3.5 eV, so that the energy difference between the bonding band and the conduction-band minimum is, like ThO_2 , ~ 6 eV. Furthermore, we should expect an additional interband absorption onset in UO_2 at ~ 6 eV, resulting from transitions between the "bonding" band directly to the conduction-band minimum. This absorption onset has, indeed, been reported by Ackerman *et al.*²⁵ Thus, in the absence of the $5f$ electrons in UO_2 , we find a remarkable similarity between the electronic structures of UO_2 and ThO_2 .

ThO_2 is diamagnetic whereas UO_2 is antiferromagnetic with a Néel temperature of 30°K . It has been shown from neutron-diffraction experiments²⁶ that two highly correlated $5f$ electrons in the uranium ion are responsible for the magnetism in UO_2 . These results are consistent with the present observations, which show the $5f$ electrons well separated from the "bonding" band. UO_2 is a semiconductor in which charge transport apparently occurs via low-mobility holes. The mobile hole is formed when the "impurity" or "excess" oxygen is ionized; a uranium $5f$ electron becomes bound to the interstitial (acceptor) oxygen. Since the $5f$ electrons lie closest to E_F , less energy is needed to ionize these electrons than to ionize the "bonding" electrons. This also accounts for the fact that the magnetic susceptibility of UO_{2+x} is a strongly decreasing function of x^5 because of a dilution of the low-binding-energy $5f$ electrons on the uranium ion.

Since the photoelectron-escape depth is typically a few atomic layers,²⁷ a simple procedure is available for studying the variation of the XPS spectra

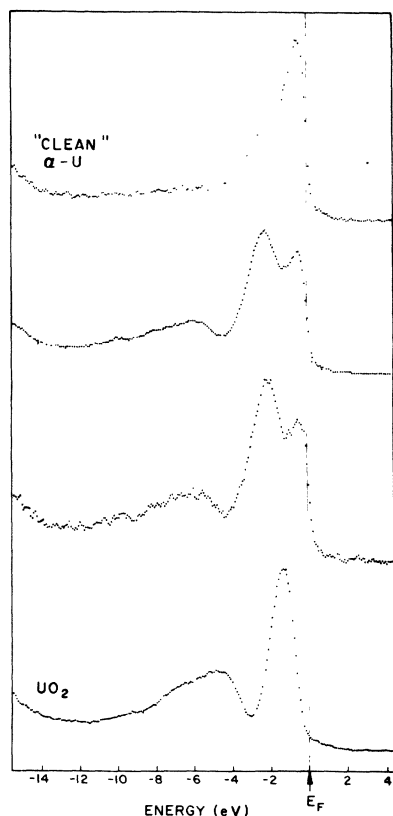


FIG. 6. XPS valence spectra of UO_2 (lower curve) and α -uranium metal (upper curve). The intermediate curves show composite spectra of thin oxide films over uranium metal.

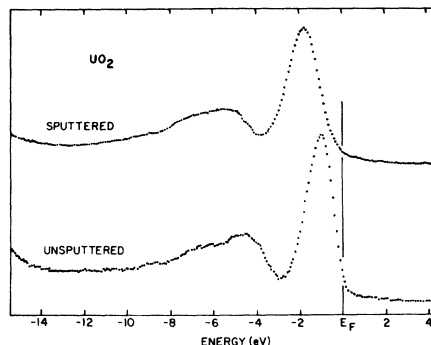


FIG. 7. Valence-band XPS spectra for a sputtered and unsputtered bulk UO_2 sample. The sputtered sample shows a Fermi-level shift.

with oxygen content in a film of UO_2 . The experiment is performed by means of sequential measurements after sputter etching with a dc argon-ion beam. Figure 6 shows several XPS spectra of an oxide film grown on a bulk α -uranium substrate. The lowest curve shows a pure oxide spectrum (the oxide film is sufficiently thick to block any contribution from the underlying substrate), and the uppermost curve shows the α -uranium XPS spectrum with a small residual oxide shoulder at 2.4 eV below E_F . As the oxide is thinned, the underlying metal valence-band structure is seen (Fig. 6, middle two curves) superimposed on the oxide spectrum. The sharp cutoff of the Fermi edge provides easy identification of a metallic contribution. Figure 6 shows that, as the oxide is thinned, the UO_2 contribution to the XPS spectrum shifts away from E_F . This shift is consistent with the interpretation that the oxide film forms as the heavily doped p -type semiconductor UO_{2+x} ($x > 0$), in which case the Fermi level is pinned to the "valence-band" edge. (The $5f$ electrons may be quite localized, in which case a band description is not appropriate.) As the film thickness decreases, the conductor becomes more nearly intrinsic (for a monolayer coverage of oxygen, one would expect no interstitial oxygen sites), with the consequence that E_F moves toward the center of the semiconducting band gap.

Supporting evidence for this interpretation is obtained by sputter etching a bulk UO_{2+x} ($x \approx 0.008$) sample. The lower curve in Fig. 7 shows the XPS spectrum before sputtering, with E_F pinned close to the "valence-band" edge. After sputtering, the entire spectrum has shifted $\sim 1\text{ eV}$ away from E_F . These results indicate that interstitial oxygen is preferentially removed from the bulk UO_{2+x} sample. The binding-energy difference between a lattice and interstitial oxygen is probably sufficiently small that, with ion bombardment, oxygen is re-

moved readily from either site. However, because of the difference in strain energy, an oxygen-ion vacancy on a lattice site is quickly filled by a nearby interstitial oxygen atom. In any case, the net effect is that after sputtering the interstitial oxygen is preferentially removed. Thus, as in the case of the oxide film, sputtering of the bulk oxide makes the surface layers sampled by the inelastically scattered photoelectrons more nearly intrinsic.

In addition to the observed spectral shifts (which are also observed in the deep-lying core states), a small broadening occurs that is probably associated with doping gradients. These results emphasize that one should proceed with caution when examining XPS core-level binding-energy shifts of semiconducting samples because the observed energies might vary significantly with impurity-doping concentration.

Conductivity measurements⁸ yield a thermal activation energy of 0.2–0.4 eV, which could result from an activated mobility (polaron model) or from an activated carrier concentration associated with ionization of deep-trap impurity levels (band model). The latter model, although it has apparently been rejected by recent workers,⁸ may be plausible since the ionization process involves the conversion of a fairly localized *f* electron on a uranium site to a *p* electron on an interstitial oxygen site, a transition that might easily require the observed activation energy.

Nagels *et al.*⁸ have shown that the Hall mobility for single-crystal UO₂ is less than 0.015 cm²/V sec at room temperature. They argue that this small mobility is evidence for nonbandlike behavior of the carriers and conclude that small-polaron theory provides a suitable description of the conduction mechanism. The XPS measurements support the contention that a band description of the carriers is inappropriate, since the 5*f* electrons responsible for the conductivity must surely be quite localized. However, it is not clear to us that a polaron model need be invoked. If, for example, we were to use the conductivity and Hall measurements reported by Nagels *et al.*, a reasonable case can be made for the deep-trap picture. From their smoothed results (oxygen concentration, conductivity, and activation energy), we compiled Table I.

The term ΔE_{pol} is the activation energy obtained by Nagels *et al.* from the expression

$$\sigma = (A/T)e^{-\Delta E_{\text{pol}}/kT}, \quad (1)$$

a formula derived from small-polaron theory. Here σ is the conductivity, T is absolute temperature, A is a constant, and k is the Boltzmann factor. However, the functional form appropriate to the deep-trap model is

$$\sigma = \sigma_0 e^{-\Delta E_g/kT}, \quad (2)$$

where σ_0 is the conductivity at T equal to infinity, and ΔE_g is the trap depth. The calculated values of ΔE_g obtained from the data of Nagels *et al.* using Eq. (2) are listed in Table I. From the oxygen excess x in UO_{2+x}, we compute the maximum carrier concentration n_{max} . The room-temperature carrier concentration n is then given by

$$n = n_{\text{max}} e^{-\Delta E_g/kT}. \quad (3)$$

Then from σ and n we compute the room-temperature mobility $\mu = \sigma/ne$. The value of μ is small and surprisingly constant as x is varied. This result is consistent with the deep-trap model. The calculated mobility is substantially larger than the upper limit obtained by Nagels *et al.* (they observed no Hall effect and report that $\mu < 0.015$ cm²/V sec). However, in view of the rather large uncertainties in the experimental values of x , ΔE_g , σ , and the degree of ionization of the interstitial oxygen, the computed μ is close to the experimental upper limit. For example, if ΔE_g were ~40% smaller, then the computed μ will be less than 0.015 cm²/V sec. Another possibility is that both n and μ can be activated, in which case the observed activation energy derived from $\sigma(T)$ is the sum of ΔE_g and ΔE_{pol} . An accurate determination of the Hall mobility might be helpful in clarifying our understanding of the conduction mechanism.

Another observation that may be helpful for choosing between the competing models is that UO₂ forms hyperstoichiometrically even when uranium metal is oxidized at room temperature. (We base this conclusion on our XPS measurements of uranium-oxide films grown at room temperature, since they show *p*-type conductivity.) Thus the 5*f* electrons that lie close to E_F must be able to interact with those interstitial oxygens even at room

TABLE I. Electrical parameters for UO₂ derived from the deep-trap model.

x	σ (Ω cm) ⁻¹	ΔE_{pol} (eV)	ΔE_g (eV)	n_{max} (cm ⁻³)	n at 290 °K (cm ⁻³)	μ (cm ² /V sec)
0.0012	10 ⁻⁵	0.286	0.306	2.7 × 10 ¹⁹	1.3 × 10 ¹⁴	0.48
0.0037	10 ⁻⁴	0.253	0.271	8.3 × 10 ¹⁹	16 × 10 ¹⁴	0.39
0.0061	10 ⁻³	0.220	0.235	13.7 × 10 ¹⁹	113 × 10 ¹⁴	0.55

temperature. (In the case of ThO_2 , on the other hand, where all thorium valence electrons are tied up in the metal-oxygen bond, interstitial oxygen is excluded from the lattice.) This would imply that the ionization energy of the oxygen acceptors might be a few tens of millielectron volts or less. Should this conclusion be correct, we would be forced to abandon the deep-trap model, perhaps in favor of small-polaron theory.

IV. SUMMARY

The valence-band electronic structure of thorium metal obtained by the XPS technique agrees quite well with the density of states from theoretical band calculations. The valence-band spectrum of α -uranium is consistent with the qualitative band structure suggested by Friedel.

Except for the existence of the $5f$ -electron spectrum in UO_2 , the ThO_2 and UO_2 valence-band spectra are nearly indistinguishable. Thus, in the absence of $5f$ electrons in UO_2 , we find a remarkable similarity between the electronic structure of the two oxides. However, the existence of $5f$ electrons in UO_2 gives rise to the most profound differences

in the physical properties between the two oxides, notably their electrical conductivity, color, and magnetism.

Based on sputtering experiments, we have concluded that UO_{2-x} is a heavily doped p -type semiconductor. Conduction in UO_2 apparently occurs via holes created by excitation of rather localized $5f$ electrons from the uranium to interstitial oxygen-acceptor sites. The strong dependence of the electrical conductivity and magnetic properties on excess oxygen concentration results from the existence of low-binding-energy $5f$ electrons in UO_2 .

With this new insight into the valence-band electronic structure in UO_2 , we have reexamined the deep-trap and small-polaron conduction models. It is our view at this time, that neither model can be ruled out.

ACKNOWLEDGMENTS

The authors would like to thank A. P. Paulikas and A. W. Mitchell for experimental assistance. Useful discussions have been had with J. E. Robinson, T. Arai, D. Y. Smith, A. J. Freeman, and C. B. Duke.

*Work performed under the auspices of the U. S. Atomic Energy Commission.

¹R. J. Elliott, in *Magnetism Properties of Rare Earth Metals* (Plenum, New York, 1972).

²A. C. Thorsen, A. S. Joseph, and L. E. Valby, *Phys. Rev.* **162**, 574 (1967).

³D. J. Boyle and A. V. Gold, *Phys. Rev. Lett.* **22**, 461 (1969).

⁴E. Ryshkewitch, in *Oxide Ceramics* (Academic, New York, 1960), p. 420.

⁵A. Arrott and J. E. Goldman, *Phys. Rev.* **108**, 948 (1957).

⁶M. J. Leask, L. E. J. Roberts, A. J. Walter, and W. P. Wolf, *J. Chem. Soc. (Lond.)* **1968**, 4788 (1963).

⁷B. T. M. Willis, *Proc. Br. Ceram. Soc.* **1**, 9 (1964).

⁸P. Nagels, J. Decreese, and M. Denayer, *J. Appl. Phys.* **35**, 1175 (1964).

⁹R. K. Willardson, J. W. Moody, and H. L. Goering, *J. Inorg. Nucl. Chem.* **6**, 19 (1958).

¹⁰S. Aronson, J. E. Rulli, and B. E. Schauer, *J. Chem. Phys.* **35**, 1382 (1961).

¹¹D. Chadwick and J. Graham, *Nat. Phys. Sci.* **237**, 127 (1972).

¹²D. Chadwick, *Chem. Phys. Lett.* **21**, 2 (1973).

¹³G. C. Allen and P. M. Tucker, *J. Chem. Soc. Dalton*, **1973**, 470 (1973).

¹⁴J. C. Fuggle, A. F. Burr, W. Lang, L. M. Watson,

and D. J. Fabian, *J. Phys. F* **4**, 335 (1974).

¹⁵The flood gun is a standard attachment for the 5950A spectrometer.

¹⁶R. P. Gupta and T. L. Loucks, *Phys. Rev. B* **3**, 1834 (1971).

¹⁷D. D. Koelling and A. J. Freeman, *Solid State Commun.* **9**, 1369 (1971).

¹⁸A. J. Freeman and D. D. Koelling, in *The Actinides: Electronic Structure and Related Properties* (Academic, New York, to be published), Vol. I, Chap. 2.

¹⁹D. A. Shirley, *Phys. Rev. B* **6**, 4709 (1972).

²⁰G. O. Arbman, D. D. Koelling, and A. J. Freeman, *Bull. Am. Phys. Soc.* **15**, 344 (1970).

²¹J. Friedel, *J. Phys. Chem. Solids* **1**, 175 (1956).

²²D. E. Eastman and M. Kuznietz, *Phys. Rev. Lett.* **14**, 846 (1971).

²³See, for example, S. Hufner and G. K. Wertheim, *Phys. Rev. B* **8**, 4857 (1973).

²⁴A. A. Sviridova and N. V. Suikovskaya, *Opt. Spectrosc.* **22**, 940 (1965), [*Opt. Spectrosc.* **22**, 509 (1965)].

²⁵R. J. Ackerman, R. J. Thorn, and G. H. Winslow, *J. Opt. Soc. Am.* **49**, 1107 (1959).

²⁶B. C. Frazer, G. Shirane, D. E. Cox, and C. E. Olsen, *Phys. Rev.* **140**, A1448 (1965).

²⁷R. G. Steinhardt, J. Hudis, and M. L. Perlman, in *Electron Spectroscopy*, edited by D. A. Shirley (North-Holland, Amsterdam, 1972), p. 557.